Optimization of the Polycondensation Stage of Poly(ethylene Terephthalate) Reactors

ANIL KUMAR,* SATYA N. SHARMA, and SANTOSH K. GUPTA,
Department of Chemical Engineering, Indian Institute of Technology, Kanpur-208,016, India

Synopsis

A general kinetic scheme for the polycondensation step of the PET formation has been used to establish the mole balance equations of various functional groups in batch reactors. An objective function has been defined which aims to attain a desired degree of polymerization in the shortest time, has a specified level of diethylene glycol group content, and minimizes the other side products. Using the control vector iteration procedure, an optimum temperature profile has been calculated. The computations suggest that a high temperature should be used initially which must be lowered as the time of reaction increases for limiting the formation of side products.

INTRODUCTION

Industrially, fiber, grade polyethylene terephthalate (PET) can be prepared either starting from dimethyl terephthalate (DMT) or terephthalic acid raw materials.[1,2] When the former is used, DMT is mixed with ethylene glycol and reacted in three stages to obtain the final polymer. In the first stage, the reaction of DMT with ethylene glycol yields mostly bis(hydroxyethyl) terephthalate (BHET)[3-6] which is further polymerized up to about 90% conversion in the second stage (which is sometimes called the polycondensation stage).[7-11] The last stage of polymerization is controlled by the rate of mass transfer of ethylene glycol from the reaction mass and is carried out in special wiped film reactors.[12-15]

The first stage polymerization has been modeled in terms of reaction between functional groups and the main reactions have been shown to consist of ester interchange, transesterification, and polycondensation reactions which can be written as follows:

Ester interchange:

$$E_m + G \underset{k_1/K_1}{\overset{k_1}{\rightleftharpoons}} E_g + M \tag{1}$$

Transesterification:

$$E_g + E_m \underset{k_2/K_2}{\overset{k_2}{\rightleftharpoons}} Z + M \tag{2}$$

Polycondensation:

$$E_g + E_g \underset{k_3/K_3}{\overset{k_3}{\rightleftharpoons}} Z + G \tag{3}$$

* To whom correspondence should be addressed.

CCC 0021 8995/84/041045-17$04.00

where E_m and E_g are the methyl ester and alcohol functional groups as explained in Table I and Z is a reacted bond. m and g stand for a molecule of methanol and ethylene glycol respectively. Since the feed to the polycondensation stage (second stage) is BHET, the first two reactions above do not occur, and the chain growth in this step occurs only by reaction (3).

In PET formation in the first as well as the second stage, the formation of side products is small, but they determine the ultimate properties of the polymer. This implies that the various side reactions which account for their formation cannot be ignored in any realistic simulation. The overall mechanism of the polycondensation stage has been given in Table I in which the formation of diethylene glycol (reactions 3a and b), acid end groups (reactions 2, 4a, and 4b) and vinyl end groups (reactions 5a and b) have been included.

In our earlier work,[6] we have carried out the optimization of the first stage of PET formation. In this, the objective function was defined to consist of maximizing the conversion of methyl ester groups E_m and simultaneously minimizing the side products E_c and E_v. It has been found that excess of diethylene glycol (E_{DT}) in the final product is undesirable because it lowers the melting point of the PET fibers; however, some amount of it (say D*) is necessary because it improves the dyeability of the polymer. Instead of posing this as a mini–max problem with constraints, the objective function was proposed to be

$$\text{minimize } [\alpha_1[E_m]^2 + \alpha_2\{[(E_{DT}) - D^*)^2 + [E_c]^2 + [E_v]^2\}] \tag{4}$$

where α_1 and α_2 are the two weighting parameters, and, by suitably adjusting the latter, the total diethylene glycol content could be forced as close to D* as one wished. We calculated optimal temperature profiles using eq. (4), and our study suggested the use of high temperatures initially to obtain high conversion of E_m initially but lower temperatures in the final phases to minimize the side product formation. High temperatures initially can either be obtained by using high pressures (about 3 atm) or use of inerts having high boiling points. In some patents,[1,16] the mixing of PET oligomers formed in the second stage have been mentioned to obtain such high temperatures.

There have been very few studies on the optimization of the polycondensation step of the PET reactors. Ravindranath and Mashelkar[8] have carried out the reactor simulation and have observed that an arbitrarily increasing temperature history gives a better reactor performance compared to an isothermal one. In their work, they have recognized the need of a systematic study on the optimization of the polycondensation step of the PET reactors.

In this work we have undertaken to optimize the polycondensation stage of PET formation or a given reactor residence time (industrial reactors usually have 2 h as residence time[8]). We have proposed a meaningful objective function for this stage and have found the optimum temperature profiles under various polymerizing conditions using the control vector iteration method. To reduce the memory space required, the entire temperature profile has been approximated by 100 piecewise continuous segments and the choice of temperature is constrained to lie between upper and lower bounds. The results of optimization once again suggest that high temperatures should be used initially and lower temperatures subsequently to minimize the formation of side products. Ravindranath and Mashelkar[8] point out that it is common industrial practice to have the reactor residence time as 2 h and vary the temperature and pressure of the

polycondensation reactors instead of operating them at constant temperature and pressure. They find the following profiles to give better reactor performance:

$$t = 290 - 50\,e^{-1.2\theta} \tag{5a}$$

and

$$P_t = 760\{e^{-1.8587\theta} + 1.776\theta^2 - 1.25270\theta^2\} \tag{5b}$$

where t is the temperature (°C), P_T the total pressure (mm Hg), and θ the residence time of the reactor (h). According to these workers, the temperature should be increased from 240°C to 285°C at the end of 2 h whereas the pressure should be reduced from 760 mm Hg to 1 mm Hg in the same duration of time. These profiles are chosen to avoid the flashing of BHET, which ultimately condenses in the vacuum lines. To avoid this, it is suggested that some inert material of high boiling point (for example, oligomers of PET formed at the end of the second stage as done for the first stage) be mixed with the BHET raw material before feeding it to the reactor.

RATES OF FORMATION OF THE VARIOUS SPECIES

For the mechanism of polymerization given in Table I, mole balance equations for various species in a batch reactor can be easily derived and are summarized in Table II. The activation energies and the frequency factors of various rate constants appearing in Table I and II are given in Table III. In the same table equilibrium constants have also been given, and these are found to be independent of temperature. The rate of formation of reacted bonds Z can also be derived from the reaction mechanism and is given by

$$\frac{d[Z]}{dt} = R_3 + R_8 - R_9 + R_{10} \tag{6}$$

where the R's above are defined in Table II. By adding eqs. (2.1)–(2.4) of Table II, one has

$$\frac{d[Z]}{dt} = \frac{1}{2}\frac{d}{dt}\left([E_g] + [E_c] + [E_v]\right) \tag{7}$$

which on integration gives [Z] at any time as

$$[Z] = \tfrac{1}{2}\{[E_g]_0 - ([E_g] + [E_c] + [E_v])\} \tag{8}$$

The polycondensation reactors are usually subjected to vacuum and the mole balance relations for condensation products can be derived as
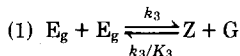
$$\frac{d[G]}{dt} = R_3 - R_7 - Q_G(t) \tag{9}$$

$$\frac{d[W]}{dt} = R_7 + R_8 - Q_W(t) \tag{10}$$
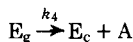
$$\frac{d[A]}{dt} = R_4 + R_{10} - Q_A(t) \tag{11}$$

KUMAR, SHARMA, AND GUPTA

TABLE I
Reaction Mechanism for the Polycondensation Stage[a]

Main reaction

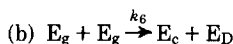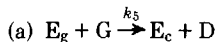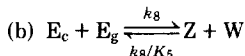(1) $E_g + E_g \underset{k_3/K_3}{\overset{k_3}{\rightleftharpoons}} Z + G$
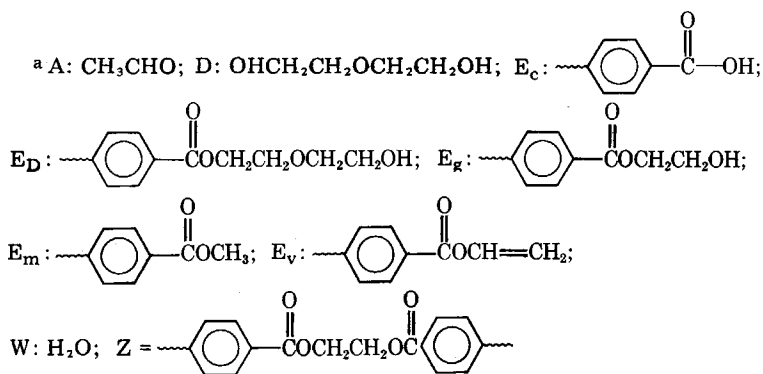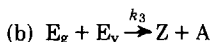
Important side reactions

(2) Acetaldehyde formation

$E_g \xrightarrow{k_4} E_c + A$

(3) Diethylene glycol formation

(a) $E_g + G \xrightarrow{k_5} E_c + D$

(b) $E_g + E_g \xrightarrow{k_6} E_c + E_D$

(4) Water formation

(a) $E_c + G \underset{k_7/K_4}{\overset{k_7}{\rightleftharpoons}} E_g + W$

(b) $E_c + E_g \underset{k_8/K_5}{\overset{k_8}{\rightleftharpoons}} Z + W$

(5) Vinyl group formation

(a) $Z \xrightarrow{k_9} E_c + E_v$

(b) $E_g + E_v \xrightarrow{k_3} Z + A$

[a] A: CH_3CHO; D: $OHCH_2CH_2OCH_2CH_2OH$; E_c: ⌬ —C(=O)—OH;

E_D: ⌬ —$COCH_2CH_2OCH_2CH_2OH$; E_g: ⌬ —$COCH_2CH_2OH$;

E_m: ⌬ —$COCH_3$; E_v: ⌬ —$COCH=CH_2$;

W: H_2O; Z = ⌬ —$COCH_2CH_2OC$— ⌬
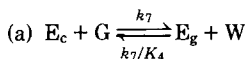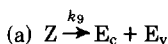
where $Q_G(t)$, $Q_W(t)$, and $Q_A(t)$ are the molar flow rates of ethylene glycol, water, and acetaldehyde, respectively, in the vapor leaving the reactor. On examining the reaction mechanism of Table I and eqs. (2.1) and (2.6) of Table II, it can be inferred that the rate of depletion of E_g is the highest when the concentration of ethylene glycol in the reaction mass is zero. Since R_3 [eq. (2.6) of Table II] is found to decrease linearly as [G] is increased, it implies that the reactor pressure should be such that the [G] in the reaction mass should be zero. Under such operating conditions, [W] as well as [A] in the reaction mass should also be zero

TABLE II
Rates of Formation of Various Functional Groups in the Polycondensation Stage

$$\frac{d[E_g]}{dt} = 2R_3 - R_4 - R_5 - R_6 + R_7 - R_8 - R_{10} \tag{2.1}$$

$$\frac{d[E_c]}{dt} = R_4 + R_5 + R_6 - R_7 - R_8 + R_9 \tag{2.2}$$

$$\frac{d[E_v]}{dt} = R_9 - R_{10} \tag{2.3}$$

$$\frac{d[E_{DT}]}{dt} = R_5 + R_6 \tag{2.4}$$

where

$$[E_{DT}] = [D] + [E_D] \tag{2.5}$$

$$R_3 = k_3 \left([E_g]^2 - \frac{4[Z][G]}{K_3} \right) \tag{2.6}$$

$$R_4 = k_4[E_g] \tag{2.7}$$

$$R_5 = 2k_5[E_g][G] \tag{2.8}$$

$$R_6 = 2k_6[E_g]^2 \tag{2.9}$$

$$R_7 = k_7 \left(2[E_c][G] - \frac{[E_g][W]}{K_4} \right) \tag{2.10}$$

$$R_8 = k_8 \left([E_c][E_g] - \frac{2[Z][W]}{K_5} \right) \tag{2.11}$$

$$R_9 = k_9[Z] \tag{2.12}$$

$$R_{10} = k_3[E_v][E_g] \tag{2.13}$$

because water and acetaldehyde have considerably higher vapour pressures compared to ethylene glycol. To maintain [G], [W], and [A], Q_G, Q_W, and Q_A in eqs. (9)–(11) should be equal to the rates of their accumulation

$$\frac{d[G]}{dt} = 0 \tag{12a}$$

$$\frac{d[W]}{dt} = 0 \tag{12b}$$

and

$$\frac{d[A]}{dt} = 0 \tag{12c}$$

FORMULATION OF THE OPTIMIZATION PROBLEM OF POLYCONDENSATION REACTORS

For a given residence time and pressure of the reactor, the temperature remains as the only variable that can be chosen arbitrarily. Usually the polymerization must be carried up to a certain molecular weight, μ_{nd}, such that the overall re-

TABLE III
Temperature Dependence of Various Rate and Equilibrium Constants Appearing in Tables I and II

	k_3	k_4	k_5	k_6	k_7	k_8	k_9
Activation energy (kcal/mol)	18.5	29.8	29.8	29.8	17.6	17.6	37.8
Frequency factor (L/mol·min)	6.8×10^5	4.16×10^{7} [a]	4.16×10^7	4.16×10^7	1.04×10^6	1.04×10^6	3.6×10^9
Equilibrium constant	$K_3 = 0.5$	—	—	—	$K_4 = 2.5$	$K_5 = 1.25$	—

[a] Units in min^{-1}.

action remains in the reaction-controlled region. Beyond μ_{nd}, the rate limiting step in the polymerization is the removal of the condensation product, and it is more efficient to carry the polymerization in wiped-film reactors.[14,16] It is therefore desired that the temperature history be chosen such that the average molecular weight, μ_n, of the polymer formed approaches μ_{nd}, simultaneously minimizing the side products, $[E_c]$ and $[E_v]$, in the reaction mass. It has been argued earlier that some amount of diethylene glycol (D*) is desirable. The objective function, I, that would attempt to achieve these in the best manner can be written as

$$\text{minimize } I = \alpha_1 |([E_{DT}] - D^*)| + \int_0^{t_f} \left\{ \frac{\alpha_2}{\mu_{nd}} \left(\frac{[E_g]_0}{[E_g]} - \mu_{nd} \right)^2 \right.$$
$$\left. + \alpha_3([E_c]^2 + [E_v]^2) \right\} dt \quad (13)$$

Ray[17] and Ray and Szekely[18] observe that this form of the objective function would achieve the desired average molecular weight, μ_{nd}, in the shortest time, even though the reactor residence time t_f in this formulation is assumed to be constant. This means that once the desired goal is achieved (in $t < t_f$) there are very small changes in the reaction mass after this time. Therefore, the choice of the objective function given in eq. (13) gives the minimum desired t_f. Our computation results on the polycondensation reactor show exactly this, and, this way, it leads to saving of considerable computational time.

An objective function of the form written in eq. (13) allows a considerable flexibility in the optimal design of the reactor. It would bring the average chain length of the polymer and $[E_{DT}]$ close to (but not necessarily equal to) the desired values, simultaneously minimizing $[E_c]$ and $[E_v]$. In actual practice, a small deviation in μ_n and $[E_{DT}]$ can always be tolerated without jeopardizing the physical properties of the polymer, at least in the design of *new* reactors when a greater degree of flexibility is available.

The Hamiltonian H can now be written as

$$H = \frac{\alpha_2}{\mu_{nd}} \left(\frac{[E_g]_0}{[E_g]} - \mu_{nd} \right)^2 + \alpha_3([E_c]^2 + [E_v]^2)$$
$$+ \lambda_1 (-2R_3 - R_4 - R_5 - R_6 + R_7 - R_8 - R_{10})$$
$$+ \lambda_2(R_4 + R_5 + R_6 + R_7 - R_8 + R_9) + \lambda_3(R_5 + R_6) + \lambda_4(R_9 - R_{10}) \quad (14)$$

where λ_1–λ_4 are the adjoint variables which are time-dependent only and are determined by

$$-\frac{d\lambda_1}{dt} = \frac{\partial H}{\partial [E_g]} \quad (15a)$$

$$-\frac{d\lambda_2}{dt} = \frac{\partial H}{\partial [E_c]} \quad (15b)$$

$$-\frac{d\lambda_3}{dt} = \frac{\partial H}{\partial [E_{DT}]} \quad (15c)$$

$$-\frac{d\lambda_4}{dt} = \frac{\partial H}{\partial [E_v]} \quad (15d)$$

TABLE IV
Equations Governing Adjoint Variables

$$-\frac{d\lambda_1}{dt} = \frac{\partial H}{\partial[\mathrm{E_g}]} = \lambda_1\left(-4k_3[\mathrm{E_g}] - 8k_3[\mathrm{G}] - k_4 - 2k_5[\mathrm{G}]\right.$$

$$-2k_6[\mathrm{E_g}] - (k_7[\mathrm{W}]/K_4) - k_8[\mathrm{E_c}] - \frac{k_8[\mathrm{W}]}{K_5} - k_3[\mathrm{E_v}]\Bigg)$$

$$+ \lambda_2(k_4 + 2k_5[\mathrm{G}] + 2k_6[\mathrm{E_g}] + (k_7[\mathrm{W}]/K_4)$$

$$- k_8[\mathrm{E_c}] - (k_8[\mathrm{W}]/K_5) - k_9/2.0)$$

$$+ \lambda_3(2k_5[\mathrm{G}] + 2k_6[\mathrm{E_g}]) + \lambda_4(-k_9/2 + k_3[\mathrm{E_v}])$$

$$- 2(\alpha_2/10.0)([\mathrm{E_g}])_0/[\mathrm{E_g}] - 10.0/([\mathrm{E_g}]^2)$$

$$-\frac{d\lambda_2}{dt} = \frac{\partial H}{\partial[\mathrm{E_c}]} = 2\alpha_3[\mathrm{E_{DT}}] + \lambda_1\left(-4k_3[\mathrm{G}]/K_3) + 2k_7[\mathrm{W}]\right.$$

$$-k_8[\mathrm{E_g}] - (k_8[\mathrm{W}]/K_5)\Bigg) + \lambda_2\Bigg(-2k_7[\mathrm{G}]$$

$$-k_8[\mathrm{E_g}] - (k_8[\mathrm{W}]/K_5) - (k_9/2.0)\Bigg) + \lambda_4(-k_9/2.0)$$

$$-\frac{d\lambda_3}{dt} = \frac{\partial H}{\partial[\mathrm{E_{DT}}]} = 0.0$$

$$-\frac{d\lambda_4}{dt} = \frac{\partial H}{\partial[\mathrm{E_v}]} = 2\alpha_3[\mathrm{E_v}] + \lambda_1((-4k_3[\mathrm{G}]/K_3) - (k_8[\mathrm{W}]/K_5)$$

$$-k_3[\mathrm{E_g}]\Bigg) + \lambda_2\Bigg(-k_8[\mathrm{W}]/K_5 - (k_9/2.0)\Bigg)$$

$$- \lambda_4((k_9/2.0) + k_3[\mathrm{E_g}])$$

Their final values are given by

$$\lambda_3(t_f) = \alpha_1 \tag{16a}$$

$$\lambda_1(t_f) = \lambda_2(t_f) = \lambda_4(t_f) = 0 \tag{16b}$$

Equations governing the adjoint variables have been derived, and the results are summarized in Table IV.

COMPUTATIONAL SCHEME

In obtaining the optimal temperature profiles, the temperature is constrained to lie between upper and lower limits

$$450°\mathrm{K} < T < 650°\mathrm{K} \tag{17}$$

The control vector iteration procedure has been used to obtain the optimum temperature history. In this, one assumes a temperature profile $T_0(t)$, integrates the state variable equations (Table II) forward in time, integrates adjoint variable equations (Table IV) reverse in time, and finally corrects the old profile according to

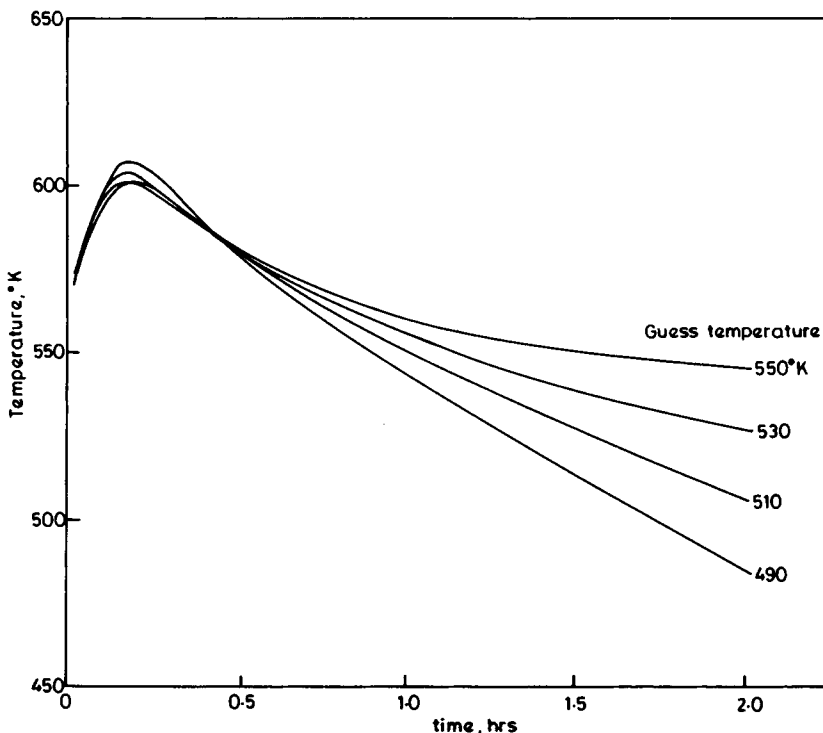$$T^{\mathrm{new}}(t) = T^{\mathrm{old}}(t) - \epsilon\left(\frac{\partial H(t)}{\partial T}\right) \tag{18}$$

Fig. 1. Optimum temperature profiles for various guess temperatures for $\alpha_1 = 1000$, $\alpha_2 = 1$, and $\alpha_3 = 0.5$.

where ϵ is assumed to be independent of time t. This completes one iteration of computation. At the optimum, one would have

$$\frac{\partial H}{\partial T} = 0 \tag{19}$$

in the unconstrained regions, which means that the change in temperature profile would not occur when the optimum is reached.

Several methods for chosing ϵ have been suggested in the literature. The one used by us[19] is a slight modification of the method suggested by Ray and Szekely.[17,18] Several ϵ values were suggested, thus generating different temperature profiles, and, after an iteration, the state variable equations are integrated forward in time and the value of the objective function calculated. The approximate value of ϵ which gives the lowest value of I is selected by inspection, and the next iteration is carried out for this value of ϵ and the corresponding temperature profile calculated using eq. (18). Our procedure requires an iterative computer terminal to be able to feed in the values of ϵ at each iteration. This procedure was needed to be adopted for this problem because the method of fitting a quadratic function[6,17,18] to the I vs. ϵ plots lead to severe numerical instabilities. Also our method was found to be considerably more rapid than that suggested by Denn,[20] which does not require an interactive computer terminal.
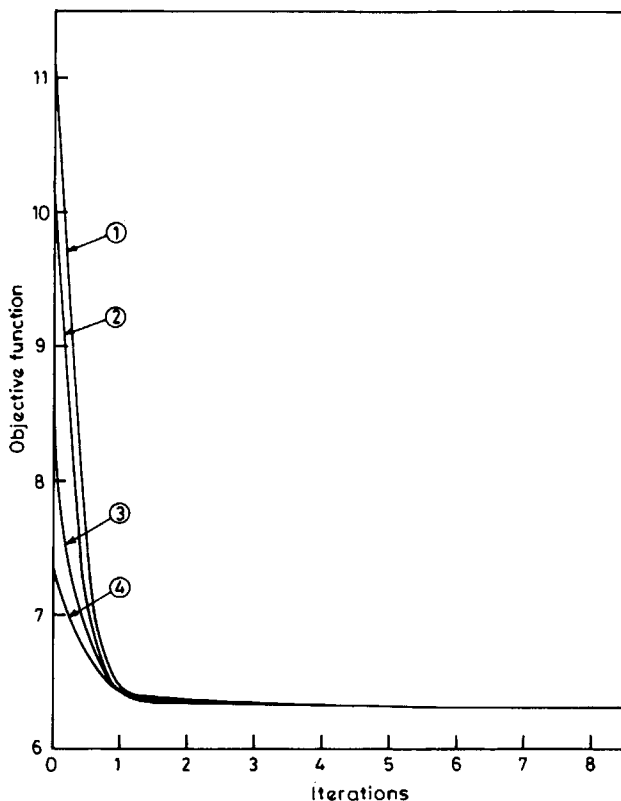
Fig. 2. The optimum values of the objective function at various iterations for various guess temperatures for $\alpha_1 = 1000$, $\alpha_2 = 1$, $\alpha_3 = 0.5$. Curve ① stands for the initial guess as 490°K, curve ② for the initial guess as 510°K, curve ③ for the initial guess as 530°K, and curve ④ for the initial guess as 550°K.

To check our computer program, we calculated the optimum temperature profile for a batch reactor carrying out the following reaction,

$$A \rightarrow B \rightarrow C$$
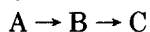
and it matched the ones given in Refs. 17 and 18. In addition to this, we calculated the stoichiometric balance and found our results consistent.

RESULTS AND DISCUSSION

The initial guess of temperature profile was given to be an isothermal one. It takes about 4 min of computation time on a DEC 1090 computer to find the optimum temperature profile. For $\alpha_1 = 1$, $\alpha_2 = 1000$, and $\alpha_3 = 0.5$, and initial isothermal guess temperatures as 490°K, 510°K, 530°K and 550°K, the optimal temperature profiles have been calculated and plotted in Figure 1. The initial portions of the profile are about the same for all, but the subsequent slow fall of temperature for the various initial guesses are found to be different. It may also be observed that the end of the temperature profiles (i.e., T at time t_f) appears to converges to the initial guess temperature. This indicates that for the
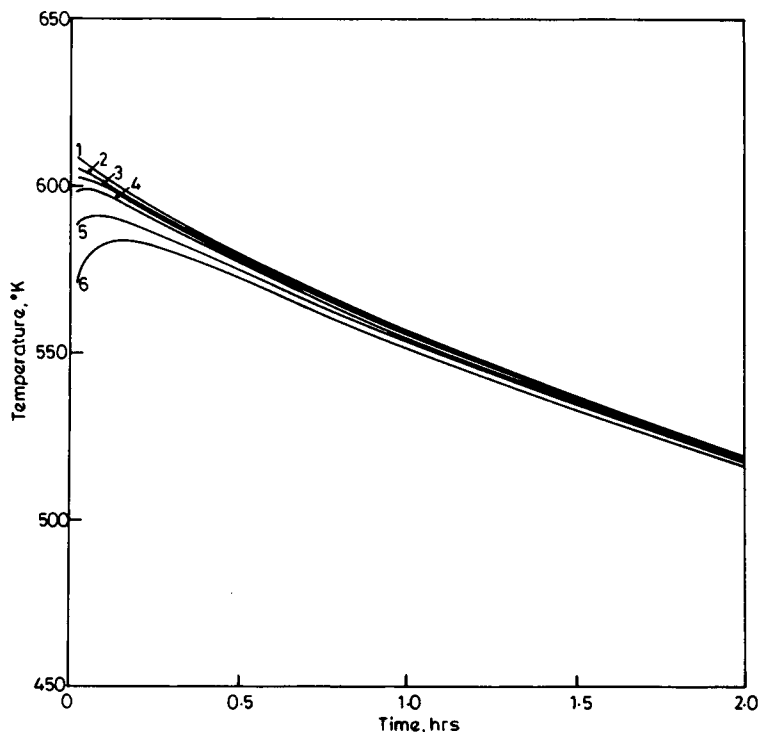
Fig. 3. Effect of α_1 on the optimum temperature profile. Values of α_1 for various curves are given in Table V.

values of α_1, α_2, and α_3 chosen for these runs, the integral part of the objective function in eq. (13) dominates over its nonintegral part. In the vector iteration procedure, $(\partial H/\partial T)$ near t_f remains close to zero and while calculating the new temperature profile using eq. (18), the end temperature is found to change negligibly from the initial guess value. In Figure 2, the change in the values of the objective function with various iterations for different guess temperatures have been given, and it is found that, for the four temperature profiles of Figure 1, the optimum values of the objective functions are almost identical. This result is consistent with observations made by Ray[18] that the convergence of the vector iteration procedure is considerably slowed down as the optimum is approached, even though the optimum value of the objective function is accurately found. Results of Figures 1 and 2 confirm that the trend of the optimum temperature profile is conserved for various initial guesses, even though there is a slight uncertainity in the exact numerical values of the optimum temperature.

To examine the effects of the weighting factors α_1, α_2, and α_3, the initial temperature has been taken as $520°K$ (isothermal). The value of μ_{nd} in eq. (13) has been taken as 10 which means that the 90% conversion of E_g groups is desired. Generally, the polycondensation reactors are subjected to high vacuum so as to drive the polymerization in the forward direction. It is therefore expected that the ethylene glycol content of the reaction mass in practice must be small. We have already discussed earlier that, at the optimum, it should be zero. Since the overall polymerization in the polycondensation reactors is reaction con-
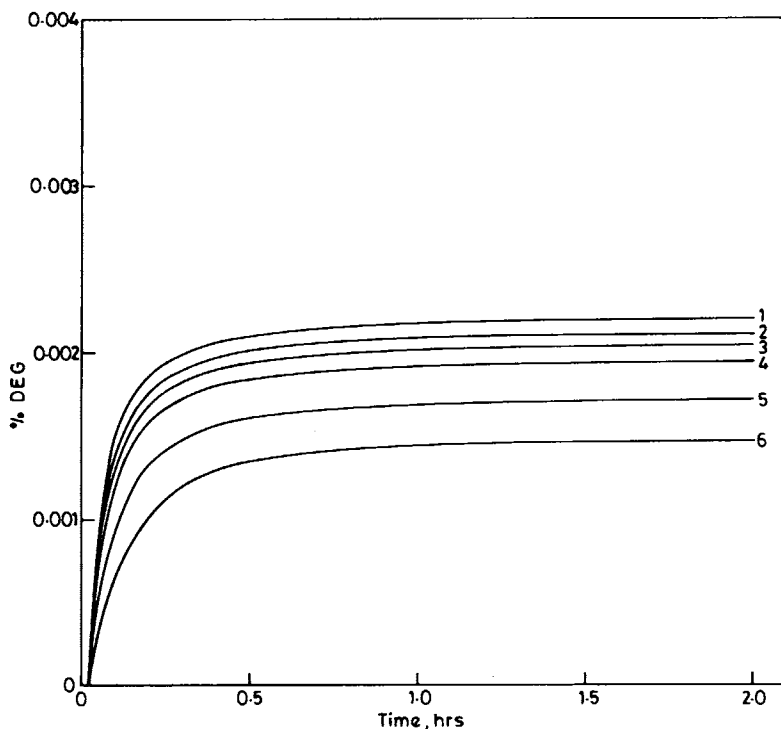
Fig. 4. Concentration of total diethylene glycol for optimum temperature profiles given in Figure 3.

trolled,[4,5,8–12] it would imply that the removal of ethylene glycol from the reaction mass is a fast process.   Therefore, without loss of any generality, the entire reaction mass can be assumed to be at some constant concentration of ethylene glycol given by the vapor liquid equilibrium existing at the reactor pressure and temperature.   In this study, [G] has been assumed to be a constant equal to 0.001. In our earlier studies on the simulation of polycondensation reactors,[8–11,14] it has been shown that the overall reaction is very close to irreversible polymerization at this value of [G].

The effect of variation of α_1 has been examined in Figures 3–6 and Table V. As α_1 is increased from 1000 to 100,000, the diethylene glycol content in the final

TABLE V
Effect of Variation of α_1 on the Optimum Temperature Profiles, Conversion, and Side Product Formation

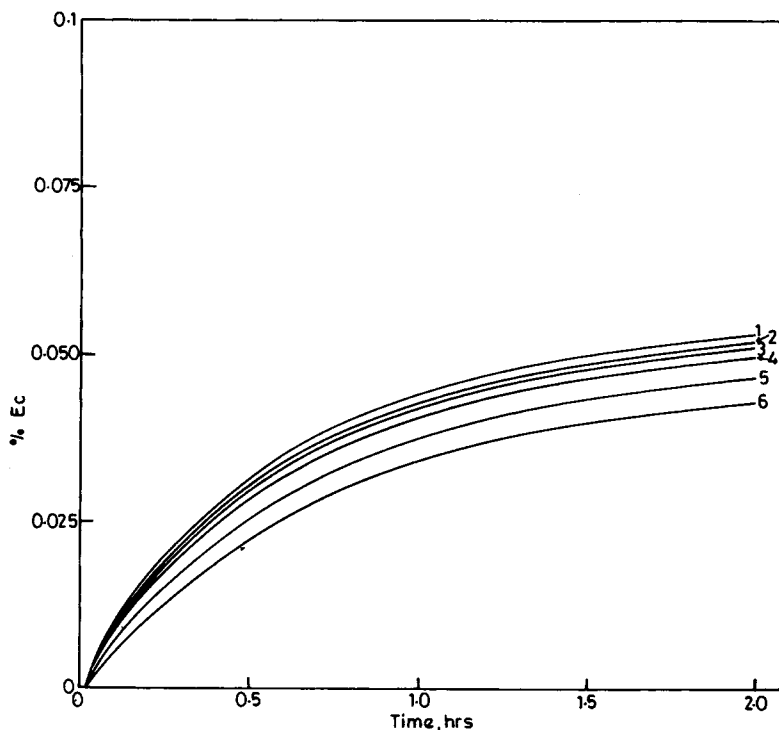| No.	α_1	Conversion %	DEG %	E_c %	E_v %
1	1000.0	90.11	0.220	5.34	0.0371
2	5000.0	89.90	0.211	5.23	0.0346
3	10,000.0	89.80	0.205	5.15	0.0329
4	20,000.0	89.60	0.195	5.00	0.0307
5	50,000.0	89.10	0.172	4.70	0.0248
6	100,000.0	88.40	0.147	4.33	0.0198

Fig. 5. [E_c] vs. reaction time for optimum temperature profiles given in Figure 3.

product reduces and this occurs at the cost of reduced conversion of E_g groups. Along with the fall in conversion, contents of E_c and E_v in the final product are also found to fall. The optimum temperature profiles have been calculated and are given in Figure 3. They are found to differ only slightly with the variation of α_1 and suggest the use of high temperature (about 330°C) initially, which should be gradually reduced as the time of polymerization increases. The contents of D, E_c, and E_v as a function of time of polymerization have been plotted in Figures 4, 5, and 6, respectively, for various values of α_1. High temperature causes high rates of their production initially, but, as the temperature is reduced, their concentrations are found to stabilize out to an asymptotic value. As opposed to this when an increasing temperature profile as suggested in eq. (5a) is used, Ravindranath and Mashelkar have shown that the production of D, E_c, and E_v accelerates near the end of the reactor. In reality, there are two ways by which high temperatures of 330°C initially can be obtained. One could either use a high pressure or a high boiling point inert to suppress the flashing of BHET monomer. High pressure cannot be used because it is necessary that ethylene glycol formed be continuously removed. In the first stage of PET formation, it is a usual practice to use PET oligomers formed at the end of the second stage as the high boiling point inert, and it is suggested that a similar scheme is adopted in the second stage to suppress the flashing of BHET and yet use high temperatures of polymerization as suggested by our studies.

The effect of variation of α_2 is studied in Figure 7 and Table VI. As the value of α_2 is increased from 0.001 to 100, the conversion is found to increase from a
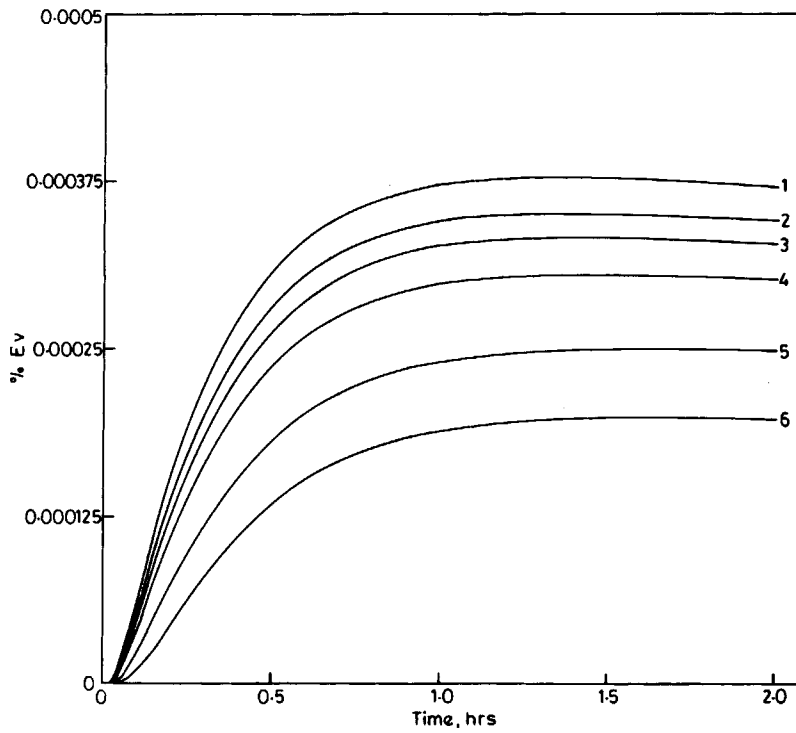
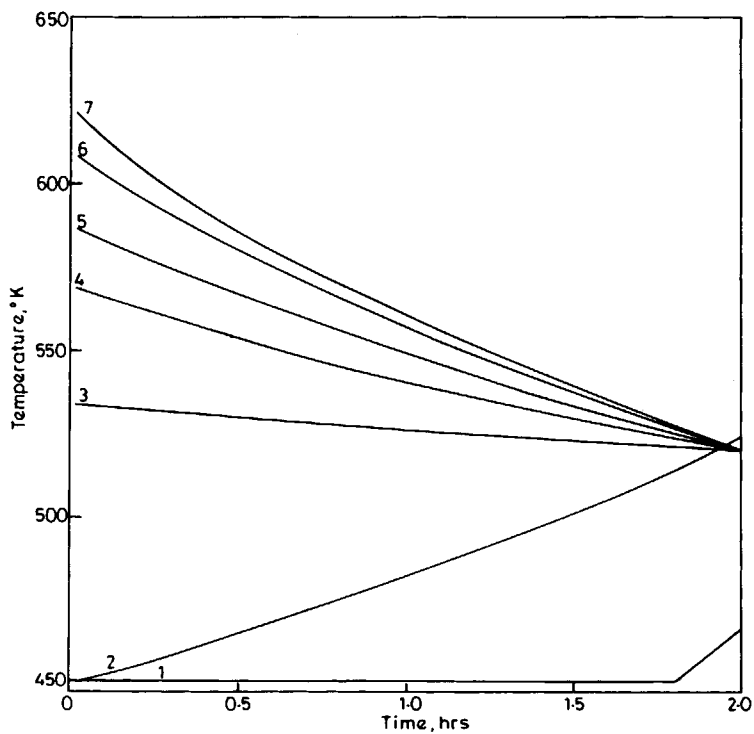Fig. 6. $[E_v]$ vs. reaction time for optimum temperature profiles given in Figure 3.

Fig. 7. Effect of α_2 on the optimum temperature profile.   Values of α_2 for various curves are given in Table VI.

TABLE VI
Effect of α_2 on the Final Conversion and Side Products

No.	α_2	α_1	α_3	Conversion %	E_c %	DEG %	E_v %
1	0.001	1000.0	20000.0	15.1	0.138	0.00153	0.86×10^{-6}
2	1.0	1000.0	20000.0	49.3	0.614	0.0158	0.197×10^{-3}
3	4.0	1000.0	20000.0	76.9	1.87	0.052	0.189×10^{-2}
4	10.0	1000.0	20000.0	84.8	3.10	0.104	0.724×10^{-2}
5	20.0	1000.0	20000.0	87.8	4.08	0.150	0.0161
6	50.0	1000.0	20000.0	90.11	5.34	0.220	0.0371
7	100.0	1000.0	20000.0	90.96	6.05	0.271	0.0563

TABLE VII
Effect of α_3 on the Final Conversion and Side Products

| No.	α_3	Conversion %	E_c %	DEG %	E_v %	Objective function
1	0.01	90.29	5.48	0.435	0.197	24.67
2	0.05	90.15	5.39	0.440	0.201	23.91
3	0.10	90.34	5.53	0.436	0.201	24.65
4	0.50	90.34	5.53	0.443	0.216	23.82
5	10.00	90.34	5.52	0.436	0.201	24.73
6	500.00	90.45	5.60	0.436	0.159	28.30
7	1000.00	90.34	5.55	0.438	0.177	31.73
8	2000.00	90.9	6.01	0.428	0.116	44.17
9	10,000.00	90.99	6.08	0.281	0.0579	125.98
10	20,000.00	90.11	5.34	0.220	0.0371	180.28
11	50,000.00	88.00	4.15	0.153	0.0169	285.03
12	100,000.00	85.00	3.15	0.104	0.00755	381.17
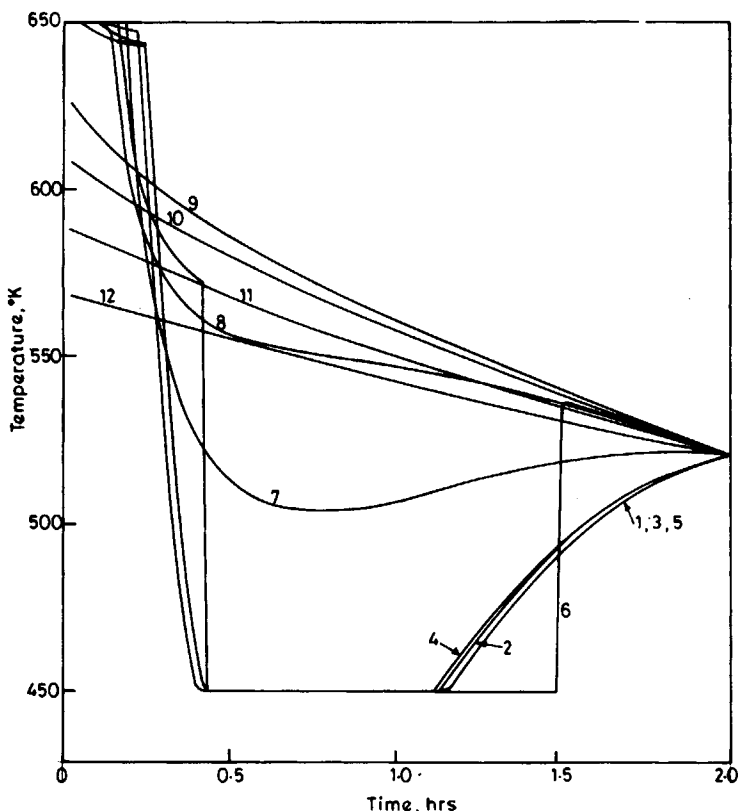
Fig. 8. Effect of α_3 on the optimum temperature profile.   Values of α_3 for various curves are given in Table VII.

low value of 15.1% to 90%, and a further increase in α_2 does not increase this conversion.   A similar trend of the formation of E_c, E_v, and D vs. reaction time is maintained as in Figures 4, 5, and 6, but their final values are found to increase as seen in Table VI.   The temperature profiles for various values of α_2 have been plotted in Figure 7 and as in Figure 3, this also suggests the use of high temperature initially which should be lowered subsequently.

As α_3 is increased from 0.01 to 10,000, the final conversion (Table VII) is little affected for this variation.   For the first five values of α_3, the concentrations of the side products are found to increase.   This occurs simply because the term $\alpha_3 ([E_c]^2 + [E_v]^2)$ is small, and the value of the objective function is determined by the first two terms in eq. (13).   As α_3 is increased beyond, conversion as well as concentrations of side products begin to fall.   In Figure 8, the optimum temperature profiles have been plotted.   The first five profiles are found to operate at the upper limit of temperature initially presumably to obtain the desired chain length average μ_{nd}.   Once the μ_{nd} is attained, the reactor temperature is allowed to fall to the lower limit where the polymerization reaction is essentially quenched.   For the values of α_3 when the conversion and concentrations of side products begin to fall, the optimization studies once again suggest the use of high temperatures initially, which must be lowered later on to reduce the formation of side products.

CONCLUSIONS

Polycondensations step of the manufacture of PET from DMT has been optimized using the vector iteration procedure suggested by Ray. The memory requirement has been reduced by approximating the temperature profile by 100 piecewise continuous segments.

Using a detailed kinetic scheme of the polycondensation step, mole balance equations for various functional groups for batch reactors have been written. An objective has been defined in which it is desired to achieve the desired molecular weight of the polymer in the shortest time simultaneously minimizing the formation of side products. This objective function involves three weighting parameters α_1, α_2, and α_3, and the optimum temperature profile is found to depend considerably on the values of these parameters. A systematic study of the effect of α_1, α_2, and α_3 on the optimum temperature profiles has been carried out in this work.

The study suggests that a high temperature must be used initially and it should be lowered to minimize the formation of side products as the time of reaction increases. The high temperature initially in practice could cause flashing of BHET monomer, and this can be suppressed either by using high pressure or using inerts of high boiling point as a diluent. High pressure cannot be used because one must remove ethylene glycol continuously to drive the overall polymerization in the forward direction. If some of the higher oligomers formed at the end of the polycondensation reactors are mixed with the BHET feed, the flashing of BHET can be suppressed as well as high temperature of polymerization initially could be realized in reality.

References

1. M. Katz, in *Polymerization Processes*, C. E. Schildknecht and I. Skeist, Eds., Wiley-Interscience, New York, 1977.
2. S. K. Gupta and A. Kumar, *Chem. Eng. Commun.*, 20 (1–2), 1 (1983).
3. J. W. Ault and D. A. Mellichamp, *Chem. Eng. Sci.*, 27, 2219 (1972).
4. K. Ravindranath and R. A. Mashelkar, *J. Appl. Polym. Sci.*, 26, 3179 (1981).
5. K. Ravindranath and R. A. Mashelkar, *J. Appl. Polym. Sci.*, 27, 471 (1982).
6. A. Kumar, V. K. Sukthankar, C. P. Vaz, and S. K. Gupta, *Polym. Eng. Sci.*, to appear.
7. J. Bjorksten, *Polyesters and Their Applications*, 1st ed., Reinhold, New York, 1960.
8. K. Ravindranath and R. A. Mashelkar, *J. Appl. Polym. Sci.*, 27, 2625 (1982).
9. A. Kumar, S. K. Gupta, B. Gupta, and D. Kunzru, *J. Appl. Polym. Sci.*, 27, 4421 (1982).
10. A. Kumar, S. K. Gupta, and N. Somu, *Polym. Eng. Sci.*, 22, 314 (1982).
11. A. Kumar, S. K. Gupta, N. Somu, and M. V. S. Rao, *Polymer*, 24, 449 (1983).
12. M. Amon and C. D. Denson, *Ind. Eng. Chem. Fundam.*, 19, 415 (1980).
13. S. K. Gupta, A. Kumar and A. Ghosh, *Ind. Eng. Chem. Fundam.*, 23, 268 (1983).
14. A. Kumar, S. K. Gupta, S. Madan, N. G. Shah, and S. K. Gupta, *Polym. Eng. Sci.*, to appear.
15. K. Ravindranath and R. A. Mashelkar, *Polym. Eng. Sci.*, 22, 628 (1982).
16. U.S. Pat. 3,496,146 (DuPont).
17. W. H. Ray, *Advanced Process Control*, McGraw-Hill, New York, 1980.
18. W. H. Ray and J. Szekely, *Process Optimization*, 1st ed., New York, 1973.
19. A. Ramagopal, A. Kumar and S. K. Gupta, *J. Appl. Polym. Sci.*, 28, 2261 (1983).
20. M. M. Denn, *Optimization by Variational Method*, 1st ed., McGraw-Hill, New York, 1969.